Modeling Nanocomposites with Ellipsoidal and Conical Inclusions by Optimized Packing

T. Romanova[1,2(✉)], A. Pankratov[1,2], I. Litvinchev[3], and E. Strelnikova[4]

[1] Department of Mathematical Modeling and Optimal Design, Institute for Mechanical Engineering Problems of the National Academy of Sciences of Ukraine, 2/10, Pozharsky Str., Kharkiv 61046, Ukraine
tarom27@yahoo.com

[2] Department of System Engineering, Kharkiv National University of Radioelectronics, 14 Nauky ave., Kharkiv 61166, Ukraine

[3] Graduate Program in Systems Engineering, Nuevo Leon State University (UANL), Monterrey, Av. Universidad s/n, Col. Ciudad Universitaria, 66455 San Nicolas de los Garza, Nuevo Leon, Mexico

[4] Department of Hydroaeromechanics of Power Machines, Institute for Mechanical Engineering Problems of the National Academy of Sciences of Ukraine, 2/10, Pozharsky Str., Kharkiv 61046, Ukraine

Abstract. In this work mathematical models of 3D representative volume elements (RVE) with systems of nanoinclusions are developed. Ellipsoidal and conical nanoinclusions of different sizes are considered in a cuboidal matrix of nanocomposites. Optimized packing is used for computational modeling of filling a given matrix with ellipsoidal and conical nanoinclusions. The proposed approach permits designing different nanoscale structures with desired properties.

Keywords: Ellipsoidal and conical nanoinclusions · Representative volume element · Packing · Phi-function technique

1 Introduction

Solid-type nanocomposites have remarkable mechanical properties and are widely used in practice in many engineering structures and systems. Taking into account diversity of material components and distribution of particles, variety of shapes and arrangements of nanoinclusions, developing new models and methods to study nanocomposites is extremely important.

Computational experiment permits a unified parameterization of elastic properties of nanocomposites in a wide spectrum of their material characteristics, geometric and surface features. Moreover, numerical simulation can replace the expensive field work and essentially reduce the scope, cost and time for experiments.

In contrast to broad experimental studies of nanocomposites and metamaterials [1–3], only a limited number of works on their static and dynamic behavior is known

J. A. Marmolejo-Saucedo et al. (Eds.): COMPSE 2020, LNICST 359, pp. 201–210, 2021.
https://doi.org/10.1007/978-3-030-69839-3_14

[4–7]. The reason is complexity of mathematical models used to describe adequately elastic properties of involved structures. In many cases these models are based on merging basic theoretical principles of continuum mechanics with molecular level descriptions. Computational nanotechnology focuses on numerical simulation in the area [4] and the results are basically related to two-dimensional configurations of the objects [8, 9].

Concerning three-dimensional configurations, they have been analyzed mainly with the assumptions of canonical single spherical particles in the nanocomposite or spherical inclusions in the periodically structured nanomaterial. In this study we consider 3D nanocomposites. Under linear elasticity assumptions, elastic and mechanical properties of composite materials and nanocomposites are considered. The non-classical boundary conditions on the interfaces are addressed to the problems [10–12]. Boundary element methods are applied to numerical solutions of the problems under consideration. The effective algorithm based on Gauss formula is proposed for the singular integrals [13, 14]. A numerical solution of the boundary integral equations is proposed with unknowns distributed on the interface surfaces only. To study size influences at micro-and-nanoscale, the Gurtin-Murdoch theory is applied for the description of nanoscale contacts between the matrix and inclusions. This results in non-classical boundary conditions at the interface surface. This surface is considered as an elastic membrane under a given surface tension and with its own elastic characteristics such as the Lame coefficients [3, 15]. The three-dimensional isotropic elasticity equations are used for Somigliana's identity [1, 16].

In what follows a cube matrix with inhomogeneity inclusions is considered. The inhomogeneities may have the form of an ellipsoid or a (truncated) cone. A representative volume element (RVE) defined by the cube matrix containing non-homogenic elements can be used to study mechanical properties of composites and nano-composites [11, 17].

In [11] expressions for integral operators were obtained, while in [13] and [3] the effective methods were elaborated for numerical integration of corresponding equations. In [3] an effective procedure was presented for estimating the effective modules of nanocomposites. Different types of inclusions were considered resulting in new nanomaterials.

Mathematical and computational models for estimating the effective modulus of nanocomposites using RVE with different mechanical and geometrical characteristics are presented in this paper. To analyze interactions of nanoinclusions in composite materials, 3D optimized packing models are used (see, e.g. [18–27]).

In the current research the phi-function technique (see, e.g. [28–34]) is used to describe placement conditions in mathematical models of filling a given volume with ellipsoidal and conical shaped nanoinclusions.

The structure of the paper is as follows. An optimized packing problem for 3D nanoinclusions and its mathematical model are presented in Sect. 2 together with modeling geometric tools. Solution strategy and computational results are given in Sect. 3, while Sect. 4 presents concluding remarks.

2 Problem Formulation

The following notations are used to formulate the packing problem. Let Ω be a cuboid of having length l, width w and height h, which are considered as variable parameters.

Let a set of nanoinclusions $\{T_i, i \in I_n = \{1, 2, \ldots, n\}\}$ has to be placed completely inside the cuboid Ω without overlaps. Each nanoinclusion T_i can take the shape of an ellipsoid or a truncated cone.

The size of each nanoinclusion T_i is assumed to be fixed. Each nanoinclusion T_i is described in a local coordinate system while a fixed coordinate system is used for the domain Ω.

The arrangement and orientation of T_i are represented by a vector (v_i, θ_i). Here the translation is defined by $v_i = (x_i, y_i, z_i)$ and rotation is represented by the vector θ_i, where $\theta_i = (\theta_i^1, \theta_i^2, \theta_i^3)$, $\theta_i^1, \theta_i^2, \theta_i^3$ are Euler angles. The nanoinclusion T_i, translated by the vector v_i and rotated by θ_i, is stated as

$$T_i(u_i) = \{p \in R^3 : p = v_i + M(\theta_i) \cdot p^0, \forall p^0 \in T_i^0\},$$

where T_i^0 is the nanoinclusion T_i without translation and rotation, $M(\theta_i)$ is a standart rotation matrix.

The problem of filling nanoinclusions into the volume can be stated as the following optimization problem:

Pack all 3D objects $T_i(u_i)$, $i \in I_n$ fully inside the cuboid Ω of minimal volume.

The following constraints have to be met in the problem:

non-overlapping nanoinclusions

$$\text{int } T_i(u_i) \cap \text{int } T_j(u_j) = \varnothing \text{ for } j > i \in I_n, \tag{1}$$

containment of nanoinclusions into the cuboid Ω

$$T_i(u_i) \subset \Omega \Leftrightarrow \text{int } T_i(u_i) \cap \text{int } \Omega^* = \varnothing \text{ for } i \in I_n, \tag{2}$$

where $\Omega^* = R^3 \backslash \text{int}\Omega$.

To describe placement constraints (1)–(2) the phi-functions and quasi-phi-functions are used.

A quasi phi-function for two 3D objects $T_i(u_i)$ and $T_j(u_j)$ is used to present the non-overlapping conditions (1).

Let $P(u_P) = \{(x, y, z)\colon \psi_P = \alpha \cdot x + \beta \cdot y + \gamma \cdot z + \mu_P \leq 0\}$ be a half-space, where $\alpha = \sin\theta_{yP}$, $\beta = -\sin\theta_{xP} \cdot \cos\theta_{yP}$, $\gamma = \cos\theta_{xP} \cdot \cos\theta_{yP}$ and $u_P = (\theta_{xP}, \theta_{yP}, \mu_P)$.

A continuous function defined by

$$\Phi'_{ij}(u_i, u_j, u_P) = \min\{\Phi^{T_iP}(u_i, u_P), \Phi^{T_jP^*}(u_j, u_P)\}, \tag{3}$$

is a quasi-phi-function for $T_i(u_i)$ and $T_j(u_j)$, where

$\Phi^{T_iP}(u_i, u_P)$ is the normalized phi-function for $T_i(u_i)$ and $P(u_P)$ is a half-space, while $\Phi^{T_jP^*}(u_j, u_P)$ is the normalized phi-function for $T_j(u_j)$ and $P^*(u_P) = R^3 \backslash \text{int } P(u_P)$.

As follows from the definition of a quasi-phi-function $\max_{u_P} \Phi'_{ij}(u_i, u_j, u_P)$ is a phi-functions of $T_i(u_i)$ and $T_j(u_j)$ and hence (1) holds if $\max_{u_P} \Phi'_{ij}(u_i, u_j, u_P) \geq 0$.

It follows from the properties of a quasi-phi-function that if $\Phi'_{ij}(u_i, u_j, u_P) \geq 0$ for some u_P, then int $T_i(u_i) \cap$ int $T_j(u_j) = \varnothing$.

To describe containment constraints (2) a phi-function for the objects $T_i(u_i)$ and Ω^* is constructed. This phi-function may be defined in the following form

$$\Phi^{T_i\Omega^*}(l, w, h, u_i) = \min\{\varphi_{ki}(l, w, h, u_i), k = 1, \ldots, 6\}, \tag{4}$$

where $\varphi_{ki}(l, w, h, u_i)$ is a phi-function for $T_i(u_i)$ and a half-space $P_k = \{(x, y, z)\colon \varphi_k \leq 0\}$, while $\varphi_k = 0$ for $k = 1, \ldots, 6$ are equations of sides of the cuboid Ω.

Quasi-phi-Function to Assure Non-overlapping Ellipsoids

Let $T_i(u_i)$ and $T_j(u_j)$ be two ellipsoids defined by corresponding semi-axes $a_i, b_i, c_i = b_i$ and $a_j, b_j, c_j = b_j$.

To describe the non-overlapping condition int $T_i(u_i) \cap$ int $T_j(u_j) = \varnothing$ in (1), a new quasi-phi-function is introduced for ellipsoids $T_i(u_i)$ and $T_j(u_j)$ in the form

$$\Phi'_{ij}(u_i, u_j, u'_{ij}) = n_{ij} \cdot (v_i^T - v_j^T) - \left\| Q^{-1}(\theta_j) \cdot \tau_j \cdot n_{ij}^T \right\| - \left\| Q^{-1}(\theta_i) \cdot \tau_i \cdot n_{ij}^T \right\|,$$

where $\tau_i = \begin{pmatrix} a_i & 0 & 0 \\ 0 & b_i & 0 \\ 0 & 0 & b_i \end{pmatrix}$, $\tau_j = \begin{pmatrix} a_j & 0 & 0 \\ 0 & b_j & 0 \\ 0 & 0 & b_j \end{pmatrix}$,

$v_i = (x_i, y_i, z_i)$, $v_j = (x_j, y_j, z_j)$, $u'_{ij} = (\theta^1_{ij}, \theta^2_{ij})$.

Values n_{ij} and $\theta^1_{ij}, \theta^2_{ij}$ are defined in the following way. A plane $L_{ij} = \{(x, y, z) : \alpha_{ij} \cdot x + \beta_{ij} \cdot y + \gamma_{ij} \cdot z + \zeta_{ij} = 0\}$ is constructed for each pair of ellipsoids. The normal vector of the plane L_{ij} is denoted by $n_{ij} = (\alpha_{ij}, \beta_{ij}) = Q(\theta_{ij})(1, 0, 0)^T$, where $Q(\theta_{ij}) = Q_2(\theta^2_{ij}) \cdot Q_1(\theta^1_{ij})$, $\alpha_{ij} = \cos\theta^1_{ij} \cdot \cos\theta^2_{ij}$, $\beta_{ij} = \cos\theta^1_{ij} \cdot \sin\theta^2_{ij}$, $\gamma_{ij} = -\sin\theta^1_{ij}$ and $\theta^1_{ij}, \theta^2_{ij}$ are angles of rotation around the OY and OZ for the plane. Thus, $L_{ij}(\theta^1_{ij}, \theta^2_{ij}, \zeta_{ij}) = \{p = (x, y, z) : n_{ij} \cdot p^T + \zeta_{ij} = 0\}$. Detailed description of the quasi-phi-functions is presented in [30, 33].

Quasi-phi-Function for Non-overlapping Truncated Cones

Each truncated cone is defined by three vectors $p_{i1} = (x_{i1}, y_{i1}, z_{i1})$, $p_{i2} = (x_{i2}, y_{i2}, z_{i2})$ and $\mathbf{n}_i = (\mathrm{n}_i^x, \mathrm{n}_i^y, \mathrm{n}_i^z)$, as well as a pair of parameters r_{i1} and r_{i2}. Here the bottom and top bases of T_i are centred at p_{i1}, p_{i2} and have radii r_{i1}, r_{i2} correspondingly, $\mathbf{n}_i$ denotes the unit vector normal to the bottom (top) base of T_i. For each circular truncated cone $r_{i1} \neq r_{i2}$ and $r_{i1} > 0, r_{i2} > 0$. The height of T_i is denoted by h_i.

A quasi phi-function for truncated cones $T_i(u_i)$ and $T_j(u_j)$ is defined in the form

$$\Phi'_{ij}(u_q, u_g, u'_{ij}) = \min\{\Phi_i(u_i, u'_{ij}), \Phi^*_j(u_j, u'_{ij})\},$$

where $\Phi_i(u_i, u'_{ij})$ is a phi-function corresponding to the object $T_i(u_i)$ and the semi-space $\tilde{P}_{ij}$, $\Phi^*_j(u_j, u'_{ij})$ is a phi-function corresponding to the object $T_j(u_i)$ and the semi-space

$\tilde{P}_{ij}^{*} = R^3 \backslash \text{int}\, \tilde{P}_{ij}$. Here the vector $u'_{ij} = (\theta_{ij}^1, \theta_{ij}^2, \mu_{ij})$ contains all auxiliary variables of the quasi phi-function Φ_{ij}^{prime} (see [30] for details).

The phi-function corresponding to the object $T_j(u_i)$ and a semi-space $\tilde{P}_{ij}^{*}$ has the form

$$\Phi_j^*(u_i, u'_{ij}) = \min\{f_1(u_i, u'_{ij}), f_2(u_i, u'_{ij})\},$$

$$f_1(u_i, u'_{ij}) = -\tilde{\mathbf{n}}_{ij} \cdot \tilde{p}_{j1} - \mu_{ij} - r_{j1}\sqrt{1 - (\tilde{\mathbf{n}}_{ij} \cdot \tilde{\mathbf{n}}_i)^2}$$

$$f_2(u_j, u'_{ij}) = -\tilde{\mathbf{n}}_{ij} \cdot \tilde{p}_{j2} - \mu_{ij} - r_{j2}\sqrt{1 - (\tilde{\mathbf{n}}_{ij} \cdot \tilde{\mathbf{n}}_i^q)^2}$$

The non-overlapping condition (1) can be represented by the inequality $\Phi'_{ij}(u_i, u_j, u'_{ij}) \geq 0$.

All variables of the problem can be grouped in the following vector: $u = (l, w, h, u_1, u_2, \ldots, u_n, \tau) \in R^{\sigma}$, where (l, w, h) is the vector of the dimensions of the container Ω; $u_i = (v_i, \theta_i) = (x_i, y_i, z_i, \theta_i^1, \theta_i^2, \theta_i^3)$ represents placement parameters for the object T_i, $i \in I_n$; τ denotes the vector of auxiliary variables u'_{ij} for $j > i \in I_n$.

The optimized packing problem may be formulated in the form

$$\min \kappa(u) \qquad \text{s.t. } u \in W\,, \tag{5}$$

$$W = \{u \in R^{\sigma}\colon \Phi'_{ij}(u_i, u_j, u'_{ij}) \geq 0, j > i \in I_n, \Phi_i(l, w, h, u_i) \geq 0, i \in I_n\}, \tag{6}$$

where $\kappa(u) = l \cdot w \cdot h$, $\Phi'_{ij}(u_i, u_j, u'_{ij})$, $\Phi'_{ij}(u_i, u_j, u'_{ij})$ is the quasi phi-function (3) defined for the pair of the 3D objects T_i and T_j (describing the non-intersection constraint (1)), $\Phi_i(l, w, h, u_i)$ is the phi-function (4) for the 3D object $T_i(u_i)$ and the object $\Omega^* = R^3 \backslash \text{int}\ \ \Omega$ (enforcing the containment constraint (2)).

Each inequality in (6) contains the phi-function and in fact is a system of inequalities involving differentiable functions. The model (5)–(6) is a continuous nonlinear non-convex programming problem. The formulation (5)–(6) is exact in the sense that it contains all solutions for the original packing problem.

3 Solution Strategy and Computational Results

The solution approach is proposed involving the main stages as follows:

Stage 1. Generating starting points feasible to (5)–(6). The homothetic transformations of objects are used to construct feasible solutions as follows. First, construct a sufficiently large container and circumscribe each nanoinclusion (3D object) by the sphere. Then randomly generate in the large container n centers for the spheres. Scale all the spheres to the full size by solving an auxiliary nonlinear programming subproblem. Form a vector of feasible translation for all nanoinclusions (3D objects). Randomly generate parameters of rotation for all 3D objects. Construct a point feasible to the problem (5)–(6) (see, e.g. [32–34] for details).

Stage 2. Minimize (locally) in the problem (5)–(6) starting from the feasible points generated at Stage 1. Here the optimization procedure described in [35] for large-scale packing problems is used. This algorithm substitutes the original problem (5)–(6) with O(n2) constraints for a sequential solution of nonlinear subproblems with (O(n)) nonlinear constraints and variables (see [32, 33] for more details).

Stage 3. The best local minimum obtained at Stage 2 is considered as a solution to the original problem (5)–(6) .

Two problem instances below illustrate the work of the proposed multistart approach. The algorithms were implemented and executed on an AMD Athlon 64 X2 5200+ computer. For NLP subproblems the IPOPT solver (https://github.com/coin-or/Ipopt) was used [36]. The sizes of the objects were defined similar to [17].

Example 1. Packing conical nanoinclusions (truncated cones):

a) $n = 35$ including 10 items with $h = 3$ nm, $r_1 = 1.2$ nm, $r_2 = 1$ nm and 25 items with $h = 2$, $r_1 = 0.6$, $r_2 = 0.5$.

The best objective function value obtained for 962.43 s. (10 starting points) is

$$\kappa(u^*) = l^* \cdot w^* \cdot h^* = 8.793475 * 6.162114 * 5.351081 = 289.95579091634.$$

b) $n = 40$ including 10 items with $h = 3$ nm, $r_1 = 1.5$ nm, $r_2 = 1$ nm and 30 items with $h = 2$, $r_1 = 0.8$, $r_2 = 0.5$.

The best objective function value found for 1187.06 s. (10 starting points) is

$$\kappa(u^*) = l^* \cdot w^* \cdot h^* = 7.579022 * 6.926660 * 7.369393 = 386.87329797418.$$

The local optimal solutions corresponding to Example 1 are shown in Fig. 1.

Example 2. Packing $n = 100$ ellipsoidal nanoinclusions (spheroids) with semi axes $a = 5$ nm, $b = 3$ nm and $c = 3$ nm.

The best objective function value found for 35548.86 s. (25 starting points) is

$$\kappa(u^*) = l^* \cdot w^* \cdot h^* = 67.982988 * 71.036815 * 61.835043 = 298619.6603799.$$

The local optimal solution for Example 2 is presented in Fig. 2.

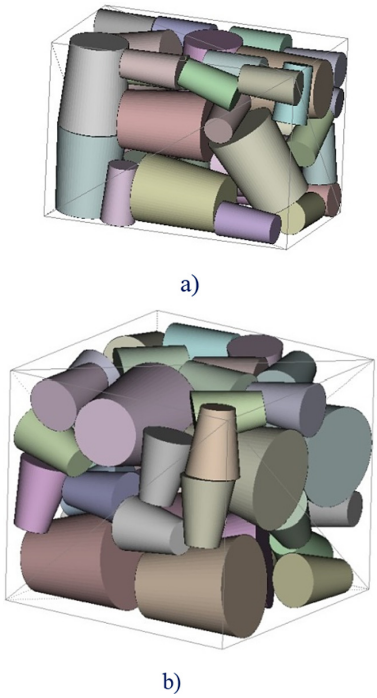

Fig. 1. Local optimal packings for conical nanoinclusions: a) $n = 35$; b) $n = 40$.

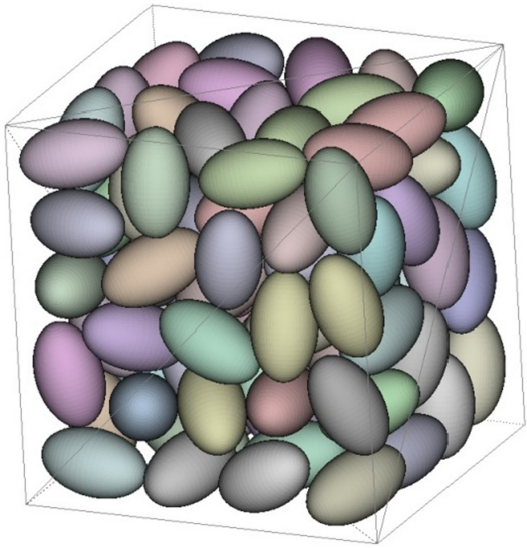

Fig. 2. Local optimal packing for $n = 100$ elliptical nanoinclusions.

4 Concluding Remarks

In this work novel mathematical models of representative volume elements with different mechanical and geometrical characteristics are proposed. To represent mutual interactions of nanoinclusions in composite materials, 3D optimized packing models are developed. Numerical experiment was conducted to illustrate the approach. Using numerical modeling instead of expensive full-scale experiments facilitates synthesis of nanocomposites with desired properties.

Simple convex (regular) shapes (ellipsoids and truncated cones) were used in this work to represent the composite matrix and nanoincusions in packing models. However, in many practical cases nanoinclusions may have irregular shapes [37–41] or can be represented as a composition of regular shapes [37]. An alternative research direction is covering complex objects by more simple shapes [42, 43] or applying other ideas for placement conditions [44]. Large dimension of the problem (5)-(6) may complicate its direct solution. Using aggregation approach [45] or decomposition [46] may help constructing low-dimensional models to get reasonable suboptimal solutions.

Acknowledgment. T. Romanova, A. Pankratov and E. Strelnikova acknowledge partial support by the "Program for the State Priority Scientific Research and Technological (Experimental) Development of the Department of Physical and Technical Problems of Energy of the National Academy of Sciences of Ukraine" (#6541230).

References

1. Barnett, A., Greengard, L.: A new integral representation for quasiperiodic fields and its application to two-dimensional band structure calculations. J. Comput. Phys. **2**, 6898–6914 (2010)
2. Kushch, V., Mogilevskaya, S., Stolarski, H., Crouch, S.: Elastic fields and effective moduli of particulate nanocomposites with the Gurtin-Murdoch model of interfaces. Int. J. Solids Struct. **50**, 1141–1153 (2013)
3. Mykhas'kiv, V., Stasyuk, B.: Effective elastic properties of 3D composites with short curvilinear fibers: numerical simulation and experimental validation. Solid State Phenomena **258**, 452–455 (2017)
4. Mykhas'kiv, V., Zhbadynskyi, I., Zhang, Ch.: Dynamic stresses due to time-harmonic elastic wave incidence on doubly periodic array of penny-shaped cracks. J. Math. Sci. **203**, 114–122 (2014)
5. Miller, R., Shenoy, V.: Size-dependent elastic properties of nanosized structural elements. Nanotechnology **11**, 139–147 (2000)
6. Sigalas, M., Kushwaga, M., Economou, E., Kafesaki, M., Psarobas, I., Steurer, W.: Classical vibrational modes in phononic lattices: theory and experiment. Z. Kristallogr. **220**, 765–809 (2005)
7. Deymier, P.: Acoustic Metamaterials and Phononic Crystals, vol. 7. Springer, Berlin (2013). https://doi.org/10.1007/978-3-642-31232-8
8. Matus, V., Kunets, Y., Mykhas'kiv, V., Boström, A., Zhang, Ch.: Wave propagation in 2D elastic composites with partially debonded fibers by the null field approach. Waves Random Complex Media **19**, 654–669 (2009)

9. Fang, X., Zhang, L., Liu, J.: Dynamic stress concentration around two interacting coated nanowires with surface/interface effect. Meccanica **48**, 287–296 (2013)
10. Gnitko, V., Degtyarev, K., Naumenko, V., Strelnikova, E.: Coupled BEM and FEM analysis of fluid-structure interaction in dual compartment tanks. Int. J. Comput. Methods Exp. Meas. **6**(6), 976–988 (2018)
11. Gnitko, V., Degtyarev, K., Karaiev, A., Strelnikova, E.: Multi-domain boundary element method for axisymmetric problems in potential theory and linear isotropic elasticity. Int. J. Comput. Methods Exp. Meas. WIT Trans. Eng. Sci. **122**, 13–25 (2019)
12. Gnitko, V., Degtyariov, K., Naumenko, V., Strelnikova, E.: BEM and FEM analysis of the fluid-structure interaction in tanks with baffles. Int. J. Comput. Methods Exp. Meas. **5**(3), 317–328 (2017)
13. Gnitko, V., Degtyarev, K., Karaiev, A., Strelnikova, E.: Multi-domain boundary element method for axisymmetric problems in potential theory and linear isotropic elasticity. WIT Trans. Eng. Sci. **122**, 13–25 (2019)
14. Kushch, V., Sevostianov, I.: Effective elastic moduli of a particulate composite in terms of the dipole moments and property contribution tensors. Int. J. Solids Struct. **53**, 1–11 (2015)
15. Kushch, V.: Elastic fields and effective stiffness tensor of spheroidal particle composite with imperfect interface. Mech. Mater. **124**, 45–54 (2018)
16. Dong, C.: Boundary element analysis of nanoinhomogeneities of arbitrary shapes with surface and interface effects. Eng. Anal. Boundary Elem. **35**, 996–1002 (2011)
17. Mirkhalaf, S., Andrade Pires, F., Simoes, R.: Determination of the size of the Representative Volume Element (RVE) for the simulation of heterogeneous polymers at finite strains. Finite Elem. Anal. Des. **119**, 30–44 (2016)
18. Strelnikova, E., et al.: Optimized packings in analysis of 3D nanocomposites with inclusion systems. In: 2020 IEEE KhPI Week on Advanced Technology (KhPIWeek), Kharkiv, Ukraine, pp. 377–381 (2020). https://doi.org/10.1109/KhPIWeek51551.2020.9250142
19. Burtseva, L., Valdez Salas, B., Romero, R., Werner, F.: Recent advances on modelling of structures of multi-component mixtures using a sphere packing approach. Int. J. Nanotechnol. **13**, 44–59 (2016)
20. Liu, X., Liu, J., Cao, A., Yao, Z.: HAPE3D – a new constructive algorithm for the 3D irregular packing problem. Front. Inf. Technol. Electron. Eng. **16**(5), 380–390 (2015)
21. Duriagina, Z., Lemishka, I., Litvinchev, I., et al.: Optimized filling of a given cuboid with spherical powders for additive manufacturing. J. Oper. Res. Soc. China (2020). https://doi.org/10.1007/s40305-020-00314-9
22. Pintér, J., Kampas, F., Castillo, I.: Globally optimized packings of non-uniform size spheres in R^d: a computational study. Optim. Lett. **12**(3), 585–613 (2018)
23. Gately, R., in het Panhuis, M.: Filling of carbon nanotubes and nanofibres. Beilstein J. Nanotechnol. **6**(1), 508–516 (2015)
24. Mollon, G., Zhao, J.: 3D generation of realistic granular samples based on random fields theory and Fourier shape descriptors. Comput. Methods Appl. Mech. Eng. **279**, 46–65 (2014)
25. Ustach, V., Faller, R.: The raspberry model for protein-like particles: ellipsoids and confinement in cylindrical pores. Eur. Phys. J. Spec. Top. **225**(8–9), 1643–1662 (2016)
26. Wang, X., Zhao, L., Fuh, J.Y.H., Lee, H.P.: Effect of porosity on mechanical properties of 3D printed polymers: experiments and micromechanical modeling based on X-ray computed tomography analysis. Polymers **11**(7), 1154 (2019)
27. Zhao, C., Jiang, L., Teo, K.L.: A hybrid chaos firefly algorithm for three-dimensional irregular packing problem. J. Ind. Manag. Optim. **16**(1), 409–429 (2020)
28. Stoyan, Y., Romanova, T., Pankratov, A., Kovalenko, A., Stetsyuk, P.: Balance layout problems: mathematical modeling and nonlinear optimization. In: Fasano, G., Pintér, J.D. (eds.) Space Engineering. SOIA, vol. 114, pp. 369–400. Springer, Cham (2016). https://doi.org/10.1007/978-3-319-41508-6_14

29. Grebennik, I.V., Kovalenko, A.A., Romanova, T.E., Urniaieva, I.A., Shekhovtsov, S.B.: Combinatorial configurations in balance layout optimization problems. Cybern. Syst. Anal. **54**(2), 221–231 (2018). https://doi.org/10.1007/s10559-018-0023-2
30. Pankratov, A., Romanova, T., Litvinchev, I.: Packing oblique 3D objects. Mathematics **8**(7), 1130 (2020)
31. Stoyan, Y., et al.: Optimized packings in space engineering applications: Part I. In: Fasano, G, Pintér, J.D. (eds.) Modeling and Optimization in Space Engineering. SOIA, vol. 144, pp. 395–437. Springer, Cham (2019). https://doi.org/10.1007/978-3-030-10501-3_15
32. Romanova, T., Bennell, J., Stoyan, Y., Pankratov, A.: Packing of concave polyhedra with continuous rotations using nonlinear optimization. Eur. J. Oper. Res. **268**(1), 37–53 (2018)
33. Romanova, T., Litvinchev, I., Pankratov, A.: Packing ellipsoids in an optimized cylinder. Eur. J. Oper. Res. **285**(2), 429–443 (2020)
34. Romanova, T., et al.: Sparsest balanced packing of irregular 3D objects in a cylindrical container Eur. J. Oper. Res. (2020) https://doi.org/10.1016/j.ejor.2020.09.021
35. Romanova, T., Stoyan, Y., Pankratov, A., Litvinchev, I., Marmolejo, J.A.: Decomposition algorithm for irregular placement problems. In: Vasant, P, Zelinka, I., Weber, G.-W. (eds.) ICO 2019. AISC, vol. 1072, pp. 214–221. Springer, Cham (2020). https://doi.org/10.1007/978-3-030-33585-4_21
36. Wächter, A., Biegler, L.T.: On the implementation of an interior-point filter line-search algorithm for large-scale nonlinear programming. Math. Program. **106**(1), 25–57 (2006)
37. Leao, A.A., Toledo, F.M., Oliveira, J.F., Carravilla, M.A., Alvarez-Valdés, R.: Irregular packing problems: a review of mathematical models. Eur. J. Oper. Res. **282**, 803–822 (2020)
38. Araújo, L.J., Özcan, E., Atkin, J., Baumers, M.: Analysis of irregular three-dimensional packing problems in additive manufacturing: a new taxonomy and dataset. Int. J. Prod. Res. **57**, 5920–5934 (2018)
39. Wang, S., Marmysh, D., Ji, S.: Construction of irregular particles with superquadric equation in DEM. Theor. Appl. Mech. Lett. **10**, 68–73 (2020)
40. Liu, X., Liu, J.-M., Cao, A.-X., Yao, Z.-L.: HAPE3D—a new constructive algorithm for the 3D irregular packing problem. Front. Inf. Technol. Electron. Eng. **16**, 380–390 (2015)
41. Garboczi, E., Bullard, J.: 3D analytical mathematical models of random star-shape particles via a combination of X-ray computed microtomography and spherical harmonic analysis. Adv. Powder Technol. **28**, 325–339 (2017)
42. Pankratov, A., Romanova, T., Litvinchev, I., Marmolejo-Saucedo, J.A.: An optimized covering spheroids by spheres. Appl. Sci. **10**(5), 1846 (2020)
43. Stoyan, Y., Romanova, T., Scheithauer, G., Krivulya, A.: Covering a polygonal region by rectangles. Comput. Optim. Appl. **48**(3), 675–695 (2011)
44. Litvinchev, I., Romanova, T., Corrales-Diaz, R., Esquerra-Arguelles, A., Martinez-Noa, A.: Lagrangian approach to modeling placement conditions in optimized packing problems. Mobile Netw. Appl. (2020). https://doi.org/10.1007/s11036-020-01556-w
45. Litvinchev, I., Rangel, S.: Localization of the optimal solution and a posteriori bounds for aggregation. Comput. Oper. Res. **26**(10–11), 967–988 (1999)
46. Litvinchev, I., Mata, M., Rangel, S., Saucedo, J.: Lagrangian heuristic for a class of the generalized assignment problems. Comput. Math Appl. **60**(4), 1115–1123 (2010)